

Research Article

Targeted Quantitative Mass Spectrometry Analysis of Protein Biomarkers From Previously Stained Single Formalin-Fixed Paraffin-Embedded Tissue Sections

Bradley L. Ackermann^a, Ryan D. Morrison^b, Salisha Hill^b, Matthew D. Westfall^b, Brent D. Butts^a, Michael D. Soper^a, Jeff A. Fill^a, Andrew E. Schade^a, Daniel C. Liebler^{b,*}, Aaron M. Gruver^{a,*}

^a Lilly Research Laboratories, Eli Lilly and Company, Indianapolis, Indiana; ^b Protypia, Inc, Nashville, Tennessee

ARTICLE INFO

Article history:

Received 20 September 2022

Revised 30 November 2022

Accepted 15 December 2022

Keywords:

formalin-fixed tissue
mass spectrometry
quantitative proteomics
single section

ABSTRACT

Formalin-fixed, paraffin-embedded tissues represent a majority of all biopsy specimens commonly analyzed by histologic or immunohistochemical staining with adhesive coverslips attached. Mass spectrometry (MS) has recently been used to precisely quantify proteins in samples consisting of multiple unstained formalin-fixed, paraffin-embedded sections. Here, we report an MS method to analyze proteins from a single coverslipped 4- μ m section previously stained with hematoxylin and eosin, Masson trichrome, or 3,3'-diaminobenzidine-based immunohistochemical staining. We analyzed serial unstained and stained sections from non-small cell lung cancer specimens for proteins of varying abundance (PD-L1, RB1, CD73, and HLA-DRA). Coverslips were removed by soaking in xylene, and after tryptic digestion, peptides were analyzed by targeted high-resolution liquid chromatography with tandem MS with stable isotope-labeled peptide standards. The low-abundance proteins RB1 and PD-L1 were quantified in 31 and 35 of 50 total sections analyzed, respectively, whereas higher abundance CD73 and HLA-DRA were quantified in 49 and 50 sections, respectively. The inclusion of targeted β -actin measurement enabled normalization in samples where residual stain interfered with bulk protein quantitation by colorimetric assay. Measurement coefficient of variations for 5 replicate slides (hematoxylin and eosin stained vs unstained) from each block ranged from 3% to 18% for PD-L1, from 1% to 36% for RB1, 3% to 21% for CD73, and 4% to 29% for HLA-DRA. Collectively, these results demonstrate that targeted MS protein quantification can add a valuable data layer to clinical tissue specimens after assessment for standard pathology end points.

© 2022 United States & Canadian Academy of Pathology. Published by Elsevier Inc. This is an open access article under the CC BY-NC-ND license (<http://creativecommons.org/licenses/by-nc-nd/4.0/>).

Introduction

Tissue samples collected as part of clinical investigation are critical to establishing disease diagnosis and selecting therapies, but collection presents a notable logistical barrier and imposes a burden on patients. Therefore, maximizing the use of these specimens is critical for appropriate access to equitable care.^{1,2}

* Corresponding authors.

E-mail addresses: daniel.liebler@protypia.com (D.C. Liebler), gruver_aaron_m@lilly.com (A.M. Gruver).



Driven by the need to stabilize tissue architecture for microscopy, biopsied tissue specimens are commonly processed for preservation and storage by formalin fixation and paraffin embedding. Formalin-fixed and paraffin-embedded (FFPE) specimens are cut into thin sections (eg, 4–5 μm) and attached to glass slides for histopathologic staining, immunohistochemical (IHC) staining, and related imaging analyses, with adhesive coverslips attached. FFPE specimens collected for clinical studies often comprise small amounts of tissue, and priority is usually given to the microscopic analyses required for routine histopathology.³ After the research study completion, these specimens are commonly archived when insufficient material remains for further investigation.

DNA and RNA biomarker measurements in FFPE have become widely used in clinical trials as part of drug development and reflect the broad availability of established next-generation sequencing platforms.^{4,5} Protein measurement in FFPE samples has historically relied on IHC analysis, which has been the clinical assay standard, despite widely acknowledged limitations, including limited availability of high-quality antibody reagents, the qualitative or semiquantitative nature of IHC measurements, and limited capacity for multiplexed protein analyses. Targeted liquid chromatography with tandem mass spectrometry (MS) (LC-MS/MS) provides superior precision and dynamic range and is not limited by the availability of antibody reagents.⁶ We and others have described the application of targeted LC-MS/MS to quantify low abundance immune checkpoint proteins and other proteins of interest in oncology multiplexed assay panels.^{7–11} In addition, reports of alternative MS techniques for protein assessment have been published.^{12,13} Targeted LC-MS/MS analyses have been performed with clinically relevant samples—typically several unstained serial FFPE sections.^{8,10,14–16} Although this sample requirement is comparable with that for next-generation sequencing analyses,^{17,18} a smaller sample input would broaden the applicability of MS analysis to clinical specimens. Moreover, an adaptation of the approach to analyze previously stained, coverslipped sections would enable the use of archival specimens, which would not be further used and potentially obviate the need for an additional biopsy.

Analysis of single, previously stained FFPE sections requires a method that can recover and extract protein without interference from the adhesive resin used to attach coverslips and that can analyze small protein amounts in single sections (typically 1–10 μg protein). In this work, we describe a proof-of-concept study for analysis of stained, coverslipped FFPE non-small cell lung cancer (NSCLC) tissue sections and test the hypothesis that targeted MS can be used to reproducibly assess single poststained sections. Using xylene to solubilize adhesive and remove coverslips, we analyzed 4 oncology-related protein biomarkers: the clinically actionable immune checkpoint programmed death-ligand 1 (PD-L1), the tumor suppressor retinoblastoma protein (RB1), the adenosine pathway enzyme ecto-5'-nucleotidase (CD73), and the type II major histocompatibility complex human leukocyte antigen, isotype DRA (HLA-DRA). These proteins were chosen to span a broad range of abundance from low (RB1 and PD-L1) to moderate (CD73) to high (HLA-DRA) and owing to their relevance as targets of translational research. We demonstrate a normalization strategy that yields acceptable measurement variation and sample comparisons between stained sections. The results demonstrated the accessibility of high-quality quantitative protein biomarker data from previously stained slides and encourage a broader pursuit of this novel approach to analyze archival tissue specimens.

Materials and Methods

Specimen Acquisition

Deidentified FFPE tissues containing adenocarcinoma of the lung ($n = 10$) were commercially acquired between 2016 and 2020 (iSpecimen). Informed consent was obtained before specimen collection. Tissue microtomy was performed immediately before experiment initiation. Clinicopathologic details of the specimens used in the study are presented in [Supplementary Table S1](#).

Histology and Immunohistochemistry

Serial sections of NSCLC were cut at 4 μm . Tissue sections were allowed to dry at the room temperature overnight. The initial set of stained NSCLC consisted of 5 tissue sections, each prepared from 10 FFPE blocks. These sections were assessed with the following: hematoxylin & eosin (H&E) (Richard-Allen Scientific); anti-CD73 (D7F9A) monoclonal antibody for IHC staining and as a negative control (Cell Signaling Technology), stained on the Ventana Medical Systems Discovery ULTRA platform (Roche Tissue Diagnostics); Masson trichrome stain, and an unstained, paraffinized, noncoverslipped control. The accuracy of the CD73 IHC assay in NSCLC was assessed using quantitative LC-MS/MS for CD73 as a gold standard ([Supplementary Fig. S1](#)). The image analysis of IHC sections was performed essentially as described.¹¹

The second set of stained NSCLC consisted of 10 slides each from 5 FFPE blocks. These sections were prepared in alternate between unstained, paraffinized, noncoverslipped, and a coverslipped H&E stain, 5 of each. Coverslips for both slide sets were attached with mounting medium (Tissue-Tek Glas Mounting Medium, Sakura Finetek). All stained tissue sections were scanned on an Aperio ScanScope AT Slide Imager (Leica Biosystems) at 40 \times magnification; images were viewed on Aperio ImageScope (v12.3.2) before MS assessments.

Sample Preparation

Coverslipped slides were placed vertically in a glass staining jar (Coplin jar) and submerged into xylene at the room temperature until the coverslip fell off (2–3 days). The material from each 4- μm tissue section was scraped from the glass slides using a clean razor blade and transferred into a polypropylene tube (Protein LoBind tubes, Eppendorf). Furthermore, tissue from the unstained, noncoverslipped slides also was scraped into the tubes, and the paraffin was removed with 3 washes of clearing medium (Sub-X, Surgipath). Then, all tissue samples were processed by rehydration, reduction and alkylation, and tryptic digestion as described previously.¹⁰ Tryptic peptides representing PD-L1 (LQDAGVYR), HLA-DRA (EDHLFR), CD73 (VIYPAVEGR), RB (TLQTDSIDSFETQR), and β -actin (ACTB) (GYSFTTTAER) were obtained as stable isotope-labeled (SIL) standards containing U-¹³C₆, U-¹⁵N₄-arginine or U-¹³C₆, U-¹⁵N₂-lysine (>95% chemical purity; >99% isotopic purity) from Vivitide. A mixture of 80 fmol of the SIL peptide standards were added to the tryptic digests, which were then fractionated by high pH reverse-phase chromatography with disposable spin columns (Pierce High pH Reversed-Phase Peptide Fractionation Kit; Thermo Scientific) as described previously.⁸ Fractions were evaporated to dryness under vacuum and redissolved in 0.1% formic acid for the LC-MS/MS analysis.

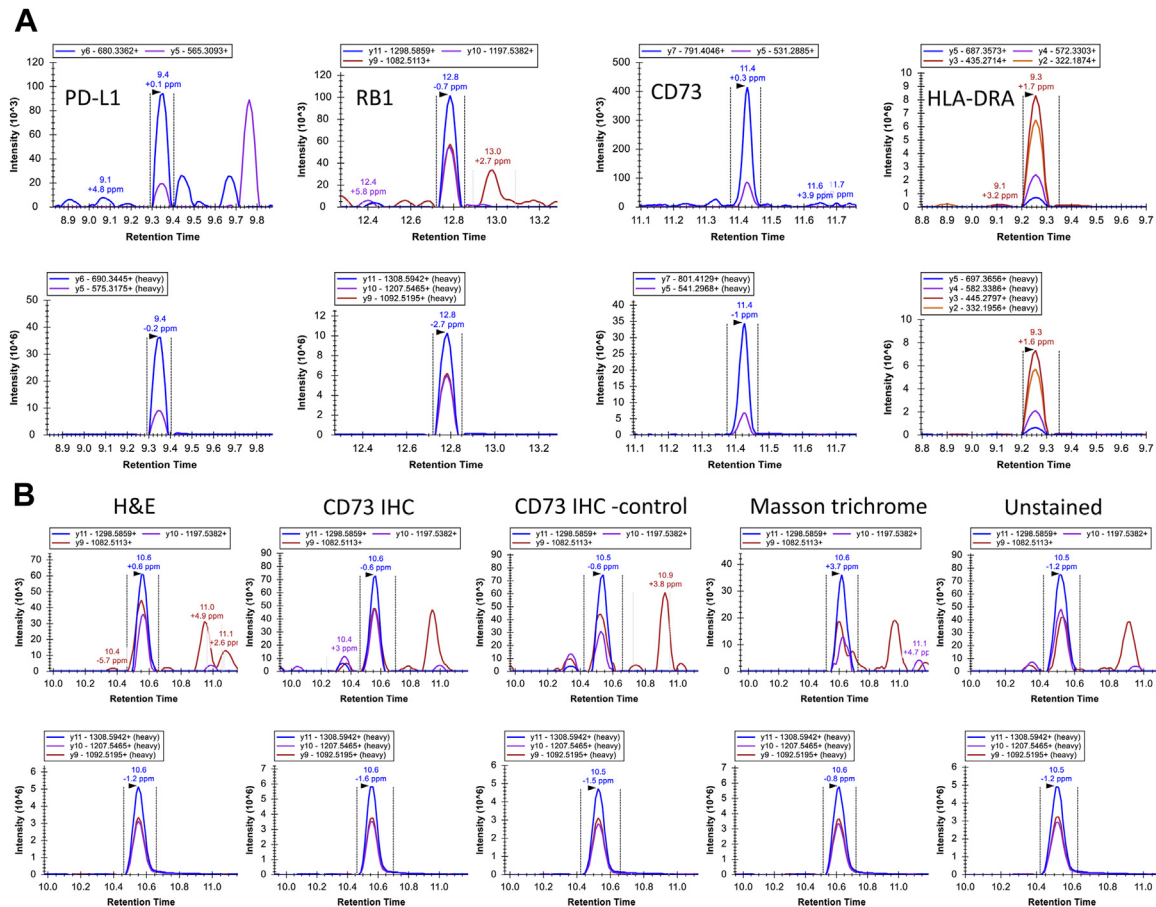


Figure 1.

(A) Liquid chromatography with tandem mass spectrometry analysis of a single H&E-stained non-small cell lung cancer section from block SR17616 T1 for PD-L1 (LQDAGVYR), RB1 (TLQTDSDSFEQTR), CD73 (VIYPAVEGR), and HLA-DRA (EDHLFR). Upper panels show transitions for unlabeled target peptide, and lower panels show transitions for corresponding peptide stable isotope-labeled standards. (B) Liquid chromatography with tandem mass spectrometry analyses of RB1 (TLQTDSDSFEQTR) in single H&E-stained, CD73 IHC, CD73 IHC negative control, Masson trichrome, and unstained non-small cell lung cancer sections from block SR18998 T4. Upper panels show transitions for unlabeled target peptide, and lower panels show transitions for corresponding peptide stable isotope-labeled standards. Colored bars represent the respective ion mass chromatograms of *y* product ions as indicated in the boxes above each stain condition. CD73, 5'-nucleotidase, ecto (NT5E); H&E, hematoxylin and eosin; HLA-DRA, major histocompatibility complex, class II, DR alpha; IHC, immunohistochemical; PD-L1, programmed cell death 1 ligand 1 (CD274); RB1, RB transcriptional corepressor 1.

Liquid Chromatography With Tandem Mass Spectrometry Analysis

Fractionated tryptic digests were analyzed by targeted MS/MS on an Exploris 480 instrument equipped with an Easy nLC 1200 liquid chromatograph and a Nanospray Flex ion source (Thermo Scientific). For the initial study, reverse-phase liquid chromatography was performed with an EasySpray C18 column (75 $\mu\text{m} \times 15\text{ cm}$, 2 μm particle size) (Thermo Scientific) eluted at 250 nL/min with a mobile phase gradient consisting of solvent A (0.1% aqueous formic acid) and solvent B (0.1% formic acid in water/acetonitrile; 1:4, vol/vol). For the second study, reverse-phase liquid chromatography was performed with an Aurora C18 column (75 $\mu\text{m} \times 15\text{ cm}$, 1.6 μm particle size) (IonOpticks) eluted at 250 nL/min with the same mobile phase gradient.

The doubly charged precursor ion for each peptide was targeted for high-energy C-trap dissociation, and full scan spectra were acquired. The acquisition method consisted of a full scan selected ion monitoring event followed by targeted MS2 scans as triggered by a scheduled inclusion list. Retention times were determined from previous analyses of synthetic peptide standards. The MS1 scan was collected at a resolution of 30,000, an automatic gain control target value of 5×10^4 , and a scan range from 375 to 1400 *m/z*. MS1 data were recorded in profile mode.

The MS1 scan was followed by targeted MS2 collision-induced dissociation scans at a resolution of 15,000, an automatic gain control target value of 5×10^4 , 1.6 *m/z* isolation window, activation Q of 0.25, and an optimized collision energy for each target of 25%. MS2 data were recorded in centroid mode.

Data were analyzed using Skyline.¹⁹ Peak areas for the 3 most intense MS/MS transitions for each peptide were extracted and summed. Quantification required at least 2 co-eluting transitions with the correct signal intensity and with mass accuracy within 10 ppm. Peptide abundance was calculated from the ratio of the peak area for the unlabeled endogenous peptide to the peak area and spike amount for the labeled internal standard. Protein abundance was inferred directly from measured peptide abundance.

Results

Targeted Mass Spectrometry Assay of Biomarker Proteins in Stained and Unstained Tissue Sections

For initial method evaluation, we prepared serial 4- μm thickness sections from 10 NSCLC FFPE tissue blocks, with 1 stained, coverslipped section each of the following: (1) H&E, (2)

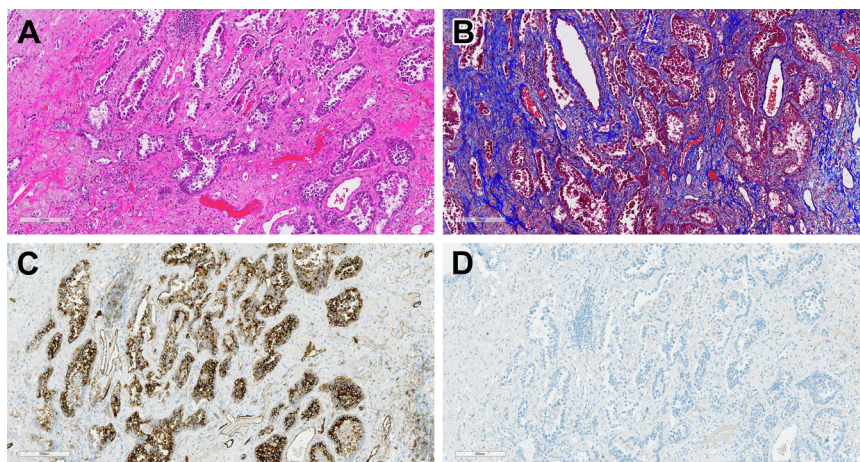


Figure 2.

Representative staining used for the quantitative liquid chromatography with tandem mass spectrometry method evaluation. (A) hematoxylin and eosin, (B) Masson trichrome, (C) CD73 immunohistochemistry, and (D) immunohistochemistry negative control. Digital images were captured using 10 \times magnification.

CD73 IHC, (3) CD73 IHC negative control, and (4) Masson trichrome and with 1 unstained, paraffinized, noncoverslipped section as an untreated control. Representative selected ion mass chromatograms are shown in Figure 1A for the tryptic peptides representing PD-L1 (LQDAGVYR), RB1 (TLQTDSIDS-FETQR), CD73 (VIYPAVEGR), and HLA-DRA (EDHLFR), from serial H&E sections from the same tumor block. The MS/MS transitions from the unlabeled peptides (upper panels) derived from the sample co-elute with those from the SIL standards (lower panels). The intensity order of the MS/MS transitions from the unlabeled peptides correspond in relative intensity to the order for the standards. Finally, the m/z value for the most intense transition differs from the theoretical value by less than 10 ppm. These criteria ensure that the measured signals are from the target peptides.

We compared signal intensities for the various stained serial sections and the unstained control section (Fig. 1B). The analysis of the RB1 TLQTDSIDSFETQR peptide yielded highly similar selected ion mass chromatograms from all specimen types. Signals for the SIL standard displayed peak intensity between 5×10^6 and 6×10^6 , and the corresponding signals for the unlabeled peptides were nearly identical, except for that from the Masson trichrome–stained slide, which was approximately half the intensity for the others.

Then, we compared measurements across a set of 50 specimens collected from 10 NSCLC FFPE tumor blocks. Each block yielded 4- μ m serial sections stained with (1) H&E, (2) CD73 IHC, (3) CD73 negative control IHC, and (4) Masson trichrome (Fig. 2) and with 1 unstained, paraffinized, noncoverslipped section. Residual stain in H&E-stained and Masson trichrome–stained slides interfered with the bicinchoninic acid (BCA) protein assay for sample protein content (not shown). However, the samples ranged from 2.58 to 42.71 mm² surface area, and previous unpublished work from our laboratory indicates that similarly sized FFPE sections yield 3 to 10 μ g protein. MS analyses detected RB1 and PD-L1 in 31 and 35 of 50 samples and CD73 and HLA-DRA in 49 and 50 of the samples, respectively (Table 1; full data are presented in Supplementary Table S2).

Variation in target protein abundances across samples ranged from 12-fold (RB1) to 85-fold (CD73). Absolute measured protein amounts ranged from 0.006 fmol (PD-L1) to 263.4 fmol (HLA-DRA). Coefficient of variation (CV) for each protein target measurement across the 5 sample types per tissue block ranged from

23% to 53% for PD-L1, from 11% to 49% for RB1, 27% to 47% for CD73, and from 29% to 69% for HLA-DRA (Supplementary Table S2).

Precision of Mass Spectrometry Measurements in Hematoxylin and Eosin–Stained and Unstained Sections With β -Actin Normalization

The high measurement variation in the initial study described may reflect variability of total sample protein input, which we were unable to control owing to interference of residual stain with the BCA protein assay. To correct for differences in protein input, we incorporated the analysis of the normalizing protein ACTB into the assay panel and analyzed a second set of 5 NSCLC samples. Ten serial sections were cut from each block, and alternate sections were stained with H&E or left unstained. The analysis of the sections was performed as the above-described study, except that a SIL standard for GYSFTTAER from ACTB was added to each sample along with the other labeled peptide standards. Quantification of all peptides was performed, and the measured values for PD-L1, RB1, CD73, and HLA-DRA were normalized to the measured value for ACTB.

Normalization of protein measurements to ACTB abundance dramatically improved measurement variation. Using non-normalized samples, CVs ranged from 11% to 53% for PD-L1, from 11% to 49% for RB1, from 21% to 54% for CD73, and from 33% to 69% for HLA-DRA (Supplementary Table S2). By contrast, CVs for 5 replicate slides (H&E stained or unstained) from each block ranged from 3% to 18% for PD-L1, from 1% to 36% for RB1, from 3% to 21% for CD73 and from 4% to 29% for HLA-DRA after normalization (Table 2;

Table 1

Range of abundances measured in 50 stained and unstained slides^a

Parameter	PD-L1	RB1	CD73	HLA-DRA
n	35	31	49	50
Low ^b	0.006	0.040	0.029	4.322
High ^b	0.199	0.472	2.505	263.4
Fold range	33	12	85	61

CD73, 5'-nucleotidase, ecto (NT5E); HLA-DRA, major histocompatibility complex, class II, DR alpha; PD-L1, programmed cell death 1 ligand 1 (CD274); RB1, RB transcriptional corepressor 1.

^a Ten non-small cell lung cancer tissue blocks were sectioned and stained/ coverslipped or unstained and analyzed for the 4 protein targets.

^b Abundances are in femtomoles.

Table 2

Reproducibility of targeted measurements of CD73, HLA-DRA, PD-L1, and RB1 with normalization to β -actin in serial hematoxylin and eosin–stained and unstained formalin-fixed paraffin-embedded sections

Sample ID		PD-L1		RB1		CD73		HLA-DRA	
		LQDAGVYR		TLQTDSIDSFETQR		VIYPAVEGR		EDHLFR	
		Unstained	H&E	Unstained	H&E	Unstained	H&E	Unstained	H&E
SR17616 T1	n	2	5	4	5	5	5	5	5
	Average	0.0210	0.0322	0.1651	0.1349	0.1806	0.1616	33.09	13.66
	%CV	5	3	19	10	21	7	18	16
SR1800193 T3	n	3	5	5	5	5	5	5	5
	Average	0.0216	0.0226	0.0835	0.0712	0.1795	0.1582	22.99	11.46
	%CV	12	11	18	7	10	7	6	29
SR19311 T2	n	2	4	5	5	5	5	5	5
	Average	0.0225	0.0187	0.0622	0.0625	0.3610	0.3976	21.40	12.97
	%CV	4	12	29	13	7	3	4	18
SR18998 T4	n	0	3	5	5	5	5	5	5
	Average	—	0.0110	0.1330	0.1025	0.1209	0.1470	6.49	3.41
	%CV	—	16	12	11	5	10	7	21
SR181142 T1	N	3	4	5	5	5	5	5	5
	Average	0.0321	0.0346	0.0824	0.0925	0.3894	0.5032	24.83	18.39
	%CV	18	3	36	1	11	7	10	5

ACTB, β -actin; CV, coefficient of variation; H&E, hematoxylin and eosin; FFPE, formalin-fixed paraffin-embedded. CD73, 5'-nucleotidase, ecto (NT5E); HLA-DRA, major histocompatibility complex, class II, DR alpha; PD-L1, programmed cell death 1 ligand 1 (CD274); RB1, RB transcriptional corepressor 1.

complete data are in [Supplementary Table S3](#)). Median CVs within blocks across all protein targets ranged from 7% to 18% for H&E slides and from 7% to 19% for unstained slides. Detection rates for the targets were similar to the initial study with PD-L1 detected in 31 samples, RB1 in 49, and CD73 and HLA-DRA in all samples. However, PD-L1 was detected in 12 H&E samples but not in the corresponding unstained sections. To determine whether there was a systematic effect of H&E staining on measured protein abundances, we compared values for the 5 H&E samples within each block with those for the 5 unstained sections ([Supplementary Table S3](#)). Only HLA-DRA was consistently detected at lower abundance in H&E-stained sections than in unstained sections with *P* values from <.0001 to .0015 (unpaired *t* test, 2-sided).

Discussion

The introduction of robust MS methods for protein quantitation in FFPE tissue makes it possible to routinely measure any protein in archival tissue. This enables a retrospective analysis of clinical specimens that may be well annotated with treatment and outcome information or with other molecular and histologic data. However, MS analyses of FFPE tissue sections described to date required multiple unstained serial sections to provide approximately 50 to 100 μ g of extracted protein for analysis. This requirement conflicts with the often limited availability of tissue sections, which are allocated to multiple diagnostic and biomarker analysis priorities. The analysis of single-stained and coverslipped FFPE sections—which would otherwise simply be archived or discarded—solves a sample availability problem and provides a means to acquire high-quality quantitation of critical biomarker proteins. In this study, we demonstrated the feasibility of such analyses for protein biomarkers of varying abundance in stained, coverslipped single FFPE sections.

We removed coverslips using xylene, which also dissolves residual adhesive that may contaminate samples if other removal methods (heating and freezing) are used. Coverslip removal in xylene typically required approximately 2 to 3 days at ambient temperature, at which time the coverslips had fallen off and residual

adhesive seemed to have been completely solubilized. After evaporation of the xylene, the samples were easily removed from the slides by scraping with a razor blade. We found that the samples were then easily rehydrated with ethanol/water washes and further processed by protein reduction, alkylation, and tryptic digestion.

The analysis of slides previously stained with H&E or Masson trichrome was complicated by the interference of residual stain with the BCA protein assay. This prevented an accurate determination of the sample protein amount taken into the analysis and normalization of the measured protein amounts to total sample protein input. Because ACTB is stably expressed across NSCLC samples, ACTB serves as a reference protein against which to normalize the abundance of other proteins and addresses an uncontrolled source of variation in the analyses. Therefore, we incorporated a targeted assay of ACTB into the assay panel. Normalization to ACTB reduced the CV for measurements of all 4 target proteins to <20% in all but 5 of the 40 sets of 5 replicate measurements per sample block.

For CD73, PD-L1, and RB1 analyses, there were no consistent, notable differences in measurements between unstained and H&E-stained samples. However, HLA-DRA measurements were consistently and notably lower in H&E-stained sections. Our data do not explain this observation, but it seems reasonable to hypothesize that H&E staining interferes with the digestion of the protein or with the recovery of the EDHLFR peptide we measured. Targeting another HLA-DRA peptide could be expected to circumvent this problem, which does not pose an obstacle to the analysis approach.

This proof-of-concept study demonstrates 2 important points. First, previously stained, coverslipped sections yield targeted MS measurements comparable with measurements from unstained FFPE sections. Second, proteins expressed over a broad abundance range can be quantified in single-stained or unstained sections. Our findings suggest the potential to substantially expand the application of targeted LC-MS/MS protein quantitation to biomarker analyses with clinical specimens. The demonstrated feasibility of protein biomarker quantitation from single, previously stained tissue sections should substantially expand the utility of MS-based tissue analyses in clinical studies. Moreover, the annotation of stained sections with a quantitative,

multiplexed protein data layer suggests an important synergy with emerging digital pathology platforms.^{20,21} Although artificial intelligence–based image analysis can advance the interpretation of tissue morphology in disease contexts, targeted MS measurements enables rigorous testing of artificial intelligence–generated models with precise, specific quantitative protein measurements. The integration of these methods can fundamentally advance the field of tissue diagnostics.

Acknowledgments

The authors wish to thank past and present members of the Clinical Diagnostics Laboratory at Eli Lilly and Company for technical assistance and critical commentary, including Patrick R. Finnegan, Darryl W. Ballard, Ling Zhang, Michael E. Hodsdon, Kelly M. Credille, and Timothy R. Holzer.

Author Contributions

B.A., A.M.G., and D.L. developed the study concept and design. R.M. and S.H. developed methodology and generated data. R.M., S.H., M.W., B.A., A.M.G., B.D.B., and D.L. provided analysis and interpretation of data. M.S. provided technical and material support. B.A., A.M.G., R.M., M.S., J.F., A.E.S., and D.L. provided writing, review, and revision of the paper. All authors read and approved the final version of the paper.

Data Availability Statement

Targeted mass spectrometry data are available through [PanoramaWeb.org](https://panoramaweb.org/p2zaj2.url) at <https://panoramaweb.org/p2zaj2.url>.

Funding

This study was supported by Eli Lilly and Company and by Prototypia, Inc.

Declaration of Competing Interest

B.L.A., B.D.B., M.D.S., J.A.F., A.E.S., and A.M.G. are employees of Eli Lilly and Company, which has therapeutic development programs related to the proteins discussed. R.D.M., S.H., M.D.W., and D.C.L. are employees of Prototypia, which provides commercial measurement services for protein biomarkers.

Ethics Approval and Consent to Participate

This study was performed in accordance with the Declaration of Helsinki.

Supplementary Material

The online version contains supplementary information available at <https://doi.org/10.1016/j.labinv.2022.100052>

References

1. Bruno DS, Hess LM, Li X, Su EW, Patel M. Disparities in biomarker testing and clinical trial enrollment among patients with lung, breast, or colorectal

- cancers in the United States. *JCO Precis Oncol.* 2022;6:e2100427. <https://doi.org/10.1200/PO.21.00427>
2. Levit LA, Peppercorn JM, Tam AL, et al. Ethical framework for including research biopsies in oncology clinical trials: American Society of Clinical Oncology Research Statement. *J Clin Oncol.* 2019;37:2368–2377. <https://doi.org/10.1200/JCO.19.01479>
3. Lim C, Sung M, Shepherd FA, et al. Patients with advanced non-small cell lung cancer: are research biopsies a barrier to participation in clinical trials? *J Thorac Oncol.* 2016;11:79–84. <https://doi.org/10.1016/j.jtho.2015.09.006>
4. Mosele F, Remon J, Mateo J, Westphalen CB, Barlesi F, Lolkema MP, et al. Recommendations for the use of next-generation sequencing (NGS) for patients with metastatic cancers: a report from the ESMO Precision Medicine Working Group. *Ann Oncol.* 2020;31:1491–1505. <https://doi.org/10.1016/j.annonc.2020.07.014>
5. Siu LL, Conley BA, Boerner S, LoRusso PM. Next-generation sequencing to guide clinical trials. *Clin Cancer Res.* 2015;21:4536–4544. <https://doi.org/10.1158/1078-0432.CCR-14-3215>
6. Gillette MA, Carr SA. Quantitative analysis of peptides and proteins in biomedicine by targeted mass spectrometry. *Nat Methods.* 2013;10:28–34. <https://doi.org/10.1038/nmeth.2309>
7. Whiteaker JR, Sharma K, Hoffman MA, et al. Targeted mass spectrometry-based assays enable multiplex quantification of receptor tyrosine kinase, MAP Kinase, and AKT signaling. *Cell Rep Methods.* 2021;1:100015. <https://doi.org/10.1016/j.crmeth.2021.100015>
8. Liebler DC, Holzer TR, Haragan A, et al. Analysis of immune checkpoint drug targets and tumor proteotypes in non-small cell lung cancer. *Sci Rep.* 2020;10:9805. <https://doi.org/10.1038/s41598-020-66902-0>
9. Zhang Q, Salzlter R, Dore A, et al. Multiplex immuno-liquid chromatography-mass spectrometry-parallel reaction monitoring (LC-MS-PRM) quantitation of CD8A, CD4, LAG3, PD1, PD-L1, and PD-L2 in frozen human tissues. *J Proteome Res.* 2018;17:3932–3940. <https://doi.org/10.1021/acs.jproteome.8b00605>
10. Morales-Betanzos CA, Lee H, Gonzalez Ericsson PI, et al. Quantitative mass spectrometry analysis of PD-L1 protein expression, N-glycosylation and expression stoichiometry with PD-1 and PD-L2 in human melanoma. *Mol Cell Proteomics.* 2017;16:1705–1717. <https://doi.org/10.1074/mcp.RA117.000037>
11. Haragan A, Liebler DC, Das DM, et al. Accelerated instability testing reveals quantitative mass spectrometry overcomes specimen storage limitations associated with PD-L1 immunohistochemistry. *Lab Invest.* 2020;100:874–886. <https://doi.org/10.1038/s41374-019-0366-y>
12. Cui M, Cheng C, Zhang L. High-throughput proteomics: a methodological mini-review. *Lab Invest.* 2022;102:1170–1181. <https://doi.org/10.1038/s41374-022-00830-7>
13. Levenson RM, Borowsky AD, Angelo M. Immunohistochemistry and mass spectrometry for highly multiplexed cellular molecular imaging. *Lab Invest.* 2015;95:397–405. <https://doi.org/10.1038/labinvest.2015.2>
14. Kennedy JJ, Whiteaker JR, Kennedy LC, et al. Quantification of human epidermal growth factor receptor 2 by immunopeptide enrichment and targeted mass spectrometry in formalin-fixed paraffin-embedded and frozen breast cancer tissues. *Clin Chem.* 2021;67:1008–1018. <https://doi.org/10.1093/clinchem/hvab047>
15. Zheng N, Taylor K, Gu H, et al. Antipeptide immunocapture with in-sample calibration curve strategy for sensitive and robust LC-MS/MS bioanalysis of clinical protein biomarkers in formalin-fixed paraffin-embedded tumor tissues. *Anal Chem.* 2020;92:14713–14722. <https://doi.org/10.1021/acs.analchem.0c03271>
16. Do M, Kim H, Yeo I, et al. Clinical application of multiple reaction monitoring-mass spectrometry to human epidermal growth factor receptor 2 measurements as a potential diagnostic tool for breast cancer therapy. *Clin Chem.* 2020;66:1339–1348. <https://doi.org/10.1093/clinchem/hvaa178>
17. Austin MC, Smith C, Pritchard CC, Tait JF. DNA yield from tissue samples in surgical pathology and minimum tissue requirements for molecular testing. *Arch Pathol Lab Med.* 2016;140:130–133. <https://doi.org/10.5858/arpa.2015-0082-OA>
18. FoundationOne CDx specimen instructions. Foundation Medicine. Accessed January 4, 2023. <https://www.foundationmedicine.com/test/foundationone-cdx>.
19. MacLean B, Tomazela DM, Shulman N, et al. Skyline: an open source document editor for creating and analyzing targeted proteomics experiments. *Bioinformatics.* 2010;26:966–968. <https://doi.org/10.1093/bioinformatics/btq054>
20. Farahmand S, Fernandez AI, Ahmed FS, et al. Deep learning trained on hematoxylin and eosin tumor region of interest predicts HER2 status and trastuzumab treatment response in HER2+ breast cancer. *Mod Pathol.* 2022;35:44–51. <https://doi.org/10.1038/s41379-021-00911-w>
21. Moutafi M, Robbins CJ, Yaghoobi V, et al. Quantitative measurement of HER2 expression to subclassify ERBB2 unamplified breast cancer. *Lab Invest.* 2022;102:1101–1108. <https://doi.org/10.1038/s41374-022-00804-9>